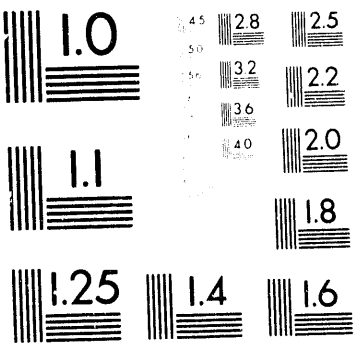
1.0
1.1
1.25
1.4
1.6
1.8
2.0
2.2
2.5
2.8
3.2
3.6
4.0
4.5
5.0
5.6

1 of 1

Patrick J. Griffin,[1] Charles V. Holm,[2] David W. Vehar,[2] and J. (Jake) G. Kelly[1]

Neutron Dosimetry with the $^{58}Ni(n,p)^{58}Co$ Reaction at Short-Decay Times[3]

REFERENCE: Griffin, P. J., Holm, C. V., Vehar, D. W., Kelly, J. G., "**Neutron Dosimetry with the $^{58}Ni(n,p)^{58}Co$ Reaction at Short-Decay Times,**" Reactor Dosimetry ASTM STP 1228. Harry Farrar IV, E. Parvin Lippincott, and John G. Williams, Eds., American Society for Testing and Materials, Philadelphia, 1994.

ABSTRACT: The $^{58}Ni(n,p)^{58}Co$ reaction is a very attractive choice for use as a neutron fluence monitor foil in reactor irradiations. The most important drawback to this reaction is the interference from the 9.15-h half-life ^{58m}Co metastable state. A methodology is presented in this paper to allow the ^{58g}Co ground-state activity to be read at short decay times and to be converted into the total ^{58t}Co activity with no significant increase in the measurement uncertainty. This methodology involves modeling the $^{58m}Co/^{58t}Co$ population ratio. Both theoretical and experimental estimates of the energy dependence of this ratio are presented. A method is presented to accurately measure this ratio. An empirical model of the energy dependence of this ratio is presented to allow simple estimates of the ratio to be made prior to a measurement.

KEYWORDS: neutron, metrology, monitor foil, $^{58}Ni(n,p)^{58}Co$, ^{58m}Co, reactor irradiation, isomer ratio

---

Nickel and sulfur are two commonly used monitor foils for reactor irradiations. The (n,p) reactions in the predominate isotopes of these materials are primarily sensitive to the neutron fluence greater than 3 MeV. Thus they are very good indicators of the reactor power without being significantly affected by changes in neutron spectrum that can be caused by presence of experiment packages. ^{58}Ni has several advantages [1] over ^{32}S that include:

- A larger (n,p) cross section. For a fast fission spectrum, the spectrum-averaged cross section for the $^{58}Ni(n,p)^{58}Co$ reaction is 1.6 that for the $^{32}S(n,p)^{32}P$ reaction.
- Gamma counting can be used on nickel foils with simple sample preparation. Beta counting is used for sulfur sensors and usually requires calibration by fluence transfer [2].
- Nickel has a long half-life that facilitates its use in high-fluence irradiations and easy foil readings at remote laboratories.
- Nickel is a corrosion- and fracture-resistant material. It can be fielded in very hostile environments.
- Nickel has a high melting point, 1452 °C, as compared to 112.8 °C for elemental sulfur. If sulfur dosimeters melt in a reactor experiment there can be environmental and health physics consequences.
- The cross section for nickel is much better characterized. It has a smaller uncertainty in the fission-spectrum-averaged cross section, i.e. 5% as compared to 19% for sulfur. The accuracy with which

---

[1]Sandia National Laboratories, Nuclear System Research, Dept. 6514, Albuquerque, NM 87185

[2]Sandia National Laboratories, Nuclear Facilities & Diagnostics, Dept. 6521, Albuquerque, NM 87185

[3]This work was performed at Sandia National Laboratories, which is operated for the U.S. Department of Energy under contract DE-AC04-76DP00789.

the $^{58}Ni(n,p)^{58}Co$ cross section is known is a strong inducement to use it as a dosimetry sensor. The measurement precision for nickel and sulfur sensors is comparable if good counting techniques are employed.

Some disadvantages to the use of nickel instead of sulfur include:

- The nickel activity is about one third that of the sulfur activity, because of the longer half-life of the nickel decay. Nickel sensors are therefore not generally useful for low fluence ($< 10^{11}$ n/cm^2) irradiations.
- For long exposures in a high thermal neutron fluence environment, $\phi_{thermal} > 10^{13}$ n/(cm^2•s), burnup of ^{58}Co can be a problem unless a boron or cadmium cover is used.
- Nickel requires a longer wait time before an activity measurement can be made, to allow interference reactions to decay. The ASTM-recommended wait time is 10 h for $^{32}S(n,p)^{32}P$ [2] and four days for $^{58}Ni(n,p)^{58}Co$ [3].

It is clear that the nickel would be the preferred monitor foil were it not for the required four days wait time before the sensor activity is read. In many experiments at research reactors this is a major disadvantage in that the experimenter and facility operators can not wait this long to determine the neutron fluence delivered to an experiment package. The primary objective of this work was to develop a methodology that would allow the use of nickel as a neutron fluence monitor at short decay times. A second objective was to quantify the error that results from the use of this methodology. As a test of its usefulness, the methodology was applied to the primary reactor facilities at Sandia National Laboratories (SNL). The procedure was defined and quantified in sufficient detail to allow its implementation at other reactor facilities.

Modeling of the ^{58m}Co-^{58g}Co Decay Systematics

Figure 1 shows the decay systematics for the $^{58}Ni(n,p)^{58}Co$ reaction. Two ^{58}Co states are populated by the (n,p) reaction; a 5^+ metastable state, ^{58m}Co, with a half-life of 9.15 h and a 2^+ ground state, ^{58g}Co, with a half-life of 70.86 days. The ^{58m}Co state decays to the ^{58g}Co ground state with an emission of a 24.9 keV gamma ray. The ^{58g}Co state decays through electron emission to the ^{58}Fe state by electron conversion and β^+ decay with the subsequent emission of a 0.8108 MeV gamma ray. This 0.8108 MeV gamma ray is typically used for measuring the activity from the $^{58}Ni(n,p)^{58}Co$ reaction. After a wait of four days following the irradiation (about ten half-lives of the ^{58m}Co state) normal decay systematics can be applied to an activity measurement. This is the standard measurement procedure [2].

The standard dosimetry procedures must be modified if an activity measurement is required prior to the four day waiting period. The following sections summarize the mathematics of decay for a parent (^{58m}Co)-daughter (^{58g}Co) system. In this discussion a subscript "a" is used to denote the parent state, and a subscript "b" for the daughter state.

Figure 1. $^{58}Ni(n,p)^{58}Co$ Decay Scheme

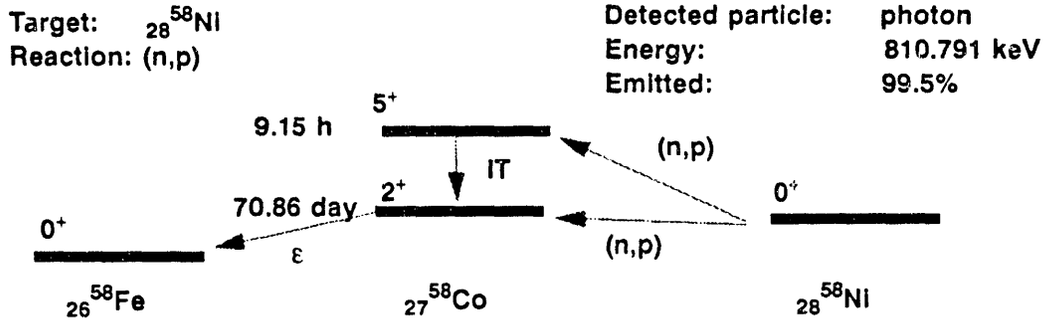

Decay After Irradiation

The following equations describe the parent-daughter decay after an irradiation:

$$\frac{d}{dt}N_a(t) = -\lambda_a \cdot N_a(t) \tag{1}$$

$$\frac{d}{dt}N_b(t) = -\lambda_b \cdot N_b(t) + \lambda_a \cdot N_a(t) \tag{2}$$

The solution to these coupled differential equations is:

$$N_a(t) = N_{a,i2} \cdot e^{-\lambda_a t} \tag{3}$$

$$N_b(t) = \frac{\lambda_a \cdot N_{a,i2}}{\lambda_b - \lambda_a} \cdot [e^{-\lambda_a t} - e^{-\lambda_b t}] + N_{b,i2} e^{-\lambda_b t} \tag{4}$$

The symbols used in these equations are defined in the **Nomenclature** section at the end of this paper.

Eqn. 4, which describes the population of the daughter state and subsequent decay, has a term that represents the feeding from the parent state and a term that represents the decay of the initial population of the state at the end of irradiation, $N_{b,i2} = N_b(t = 0)$. The time of maximum build-up in the population of the daughter state occurs at $t = t_{b,mx}$, where:

$$\frac{\partial}{\partial t}(N_b)\Big|_{t = t_{b,mx}} = 0 \tag{5}$$

This has the solution

$$t_{b,mx} = \frac{ln\left(\dfrac{\lambda_b\lambda_a N_{a,i2} - (\lambda_b - \lambda_a) \cdot \lambda_b N_{b,i2}}{\lambda_a^2 N_{a,i2}}\right)}{(\lambda_b - \lambda_a)} \tag{6}$$

Decay During Irradiation

The formulation in Eqns. 1 through 6 assumes initial populations, $N_{a,i2}$ and $N_{b,i2}$, representative of the populations at the end of irradiation. In some cases, the irradiation is not short compared to the life of the parent state (^{58m}Co in the case of nickel) and the decay during irradiation must be considered. This decay process is described by the following equations:

$$\frac{d}{dt}N_a(t_i) = P_a - \lambda_a \cdot N_a(t_i) \tag{7}$$

$$\frac{d}{dt}N_b(t_i) = P_b - \lambda_b \cdot N_b(t_i) + \lambda_a N_a(t_i) \tag{8}$$

where the solutions are:

$$N_a(t_i) = \frac{P_a}{\lambda_a}(1 - e^{-\lambda_a t_i}) \tag{9}$$

$$N_b(t_i) = \frac{P_a}{\lambda_a - \lambda_b} e^{-\lambda_a t_i} + \frac{P_a + P_b}{\lambda_b} + \frac{P_b \cdot \lambda_b - (P_a + P_b)\lambda_a}{(\lambda_a - \lambda_b)\lambda_b} \cdot e^{-\lambda_b t_i} \tag{10}$$

Decay During Counting

Since long count times (relative to τ_a, the half-life of the parent metastable state) are sometimes required for low fluence irradiations, a correction factor must be applied to a measured activity to account for decay

during counting. The normal counting-time correction, which applies to the parent state activity, is given by:

$$\zeta_a = \frac{\lambda_a T_c}{(1 - e^{-\lambda_a T_c})} \tag{11}$$

The counting-time correction for the daughter state is given by:

$$\zeta_b = \frac{\lambda_b T_c}{\left(1 - \frac{\lambda_a \Lambda}{(\lambda_b - \lambda_a)}\right)(1 - e^{-\lambda_b T_c}) + \frac{\lambda_b \Lambda}{(\lambda_b - \lambda_a)}(1 - e^{-\lambda_a T_c})} \tag{12}$$

where

$$\Lambda = \frac{\xi_p(T_w)}{(1 - \xi_p(T_w))} \tag{13}$$

If the wait time between irradiation and the start of counting, T_w, is very large relative to τ_a, and τ_a is less than τ_b, then $\xi(T_{c1}) = \xi_p(T_w) = 0$, $\Lambda = 0$, and Eqn. 12 reduces to the normal counting-time correction with a form similar to Eqn. 11.

Measurement Methodology

The decay systematics for a parent-daughter decay process can be applied to the $^{58}Ni(n,p)^{58}Co$ reaction. The following two subsections describe the methodology used to measure the $^{58m}Co/[^{58m}Co+^{58g}Co]$ isomer production ratio, η_i, at a variety of neutron sources available to the authors. η_i represents the isomer production ratio from a given neutron spectrum and does not necessarily represent the isomer state population ratio at the end of a long irradiation.

Methodology for Measuring $^{58m}Co/^{58t}Co$ Activation Ratio

1. Perform the neutron irradiation with a minimum-time exposure at a moderate fluence (~$5x10^{13}$ n/cm^2). This minimizes the irradiation decay correction and optimizes the counting statistics.
2. Count the nickel foil as soon as feasible using a counting window of 10 min. Early-time data is very important in determining the isomer ratio, so it is very desirable that the first data point be taken within 10-30 min after the irradiation. If high-purity nickel foils are not used, trace impurities can result in very large β^- or β^+ activities at early times, resulting large detector deadtime corrections.
3. Repeat the activity count over a period of 5 days using an approximately logarithmic spacing in time.
4. Use a least-squares fitting methodology to determine the isomer state populations at the end of the irradiation. The functional forms in Eqn. 3 and 4 are used with the measurements from step 3, which should include several hundred data points, to determine values for $N_{a,i2}$ and $N_{b,i2}$.
5. If a long irradiation was used (T_i>10 min), use Eqn. 9 and 10 along with the values of $N_{a,i2}$ and $N_{b,i2}$ from step 4, to apply the irradiation decay correction. This yields values for P_a and P_b where the symbol "a" represents the ^{58m}Co state and "b" represents the ^{58g}Co state.
6. The isomer production ratio is given by $\eta_i = P_a/[P_a+P_b]$. If the irradiation was short, this isomer production ratio is equal to the isomer state population ratio, $\xi(T_{i2}) = \xi_i(T_i) = N_{a,i2}/[N_{a,i2}+N_{b,i2}]$

DISCLAIMER

TABLE 1: Summary of Early-Time Nickel Decay Measurements

Reactor Environment*	Metastable Fraction	Shot Number/Date	Comment
SNL 14-MeV (14_5MEV)	0.5405	2/21/90	6.23 hour exposure, 16 data points. Corrected for decay during irradiation from 0.4316.
$S^{3}{}^{252}Cf$ (SIII28)	0.2828	4/13/90	4.067 hour exposure, 15 data points Corrected for decay during irradiation from 0.2437
SPR-III Central Cavity (SPR3CAV28-NF)	0.3170	8682 8/14/92	Spectrum characterization run for 2000 s @ 10kW Decay corrected from 0.3105
SPR-III Central Cavity (SPR3CAV28-NF)	0.3100	8894 3/3/93	2nd detailed characterization, 250 s run @ 3 kW 400 points, decay corrected from 0.3105
ACRR New Pb-B_4C Bucket (TPB13)	0.3216 0.3293 0.3228 0.3217	4/20/90	5 min irradiation in bucket, 28 data points. 4 foils tested
ACRR Central Cavity (ACF9)	0.2848	5431 8/19/92	274 data points Highly activated sample required dead-time correction from 0.3370.
* Description of environment and SNL name for the characterization of the reactor environment.			

Representative Data at Neutron Facilities

Experimental data were taken at a variety of neutron facilities and in a variety of environments as described in columns 1 and 4 of Table 1. Figure 2 shows a representative least-squares fit to the nickel foil activity using Eqn. 3 and 4. Column 2 of Table 1 shows the isomer ratios that were ascribed to these irradiations when the methodology detailed above was used.

$^{58m}Co/^{58g}Co$ Population Ratio

Theoretical Models

Theoretical modeling of the $^{58}Ni(n,p)^{58}Co$ reaction has been performed by D. Larson[4], Oak Ridge National Laboratory (ORNL), with the TNG code [4]. The TNG code uses a model for the formation of a compound nucleus and allows the ^{58m}Co state to be populated from decays from all higher lying nuclear levels, including the continuum contribution. The TNG-predicted ^{58m}Co excitation function is shown in Figure 3 by the solid curve and the filled circle data points. The ENDF/B-VI [5] ^{58}Ni cross section was not based upon the TNG model, although D. Larson was involved in its ENDF/B-VI evaluation. Since $^{58}Ni(n,p)^{58}Co$ is a reaction of primary interest to the dosimetry community, it was based on a Bayesian analysis of 12 reactions connected by ratio measurements [6]. ENDF/B-VI provides information on the $^{58}Ni(n,p)^{58t}Co$ reaction, but not on the $^{58}Ni(n,p)^{58m}Co$ reaction. A second theoretical approximation of the isomer production ratio can be obtained by taking the ratio of the TNG-predicted ^{58m}Co population to the ENDF/B-VI ^{58t}Co population. This ratio is indicated in Figure 3 by the open square data points labeled "TNG&ENDF/B-VI". The calculational uncertainty in the theory is indicative of the agreement between the "TNG" data and the "TNG&ENDF/B-VI" data.

Previous Experimental Data

A limited amount of experimental data exists on the $^{58m}Co/^{58t}Co$ isomer ratio. Passel and Heath [1] give data on the isomer ratio in the EBR-I core center and 10 in. above the center. These ratios are 0.3146 and 0.2872, respectively. These isomer ratios compare very well with the fast fission and degraded fission

[4] D. C. Larson, Oak Ridge National Laboratory, private communication to P. J. Griffin on January 29, 1990. Contents included a letter and a table extracted from TNG results dated 1/25/89.

ratios at SNL reactor facilities shown in Table 1. Experimental points for 11 energies between 1.04 MeV and 2.67 MeV have been measured by Meadows and Whalen [7]. Their work shows a lower ratio than has been observed in other fission-spectrum-averaged experiments and shows a pronounced minimum in the isomer ratio near 1.25 MeV. Figure 3 shows their data points with a filled square symbol.

Table 2: Isomer Production Data near 14 MeV

Experimenter	Energy (MeV)	$^{58m}Co/^{58t}Co$ Ratio
Hudson [9]	13.3	0.459 +/- 0.05
	14.1	0.500 +/- 0.056
	15.2	0.503 +/- 0.056
	16.0	0.489 +/- 0.068
	17.1	0.43 +/- 0.061
Decowski [13]	13.3	0.549 +/- 0.068
	14.2	0.486 +/- 0.061
	15.2	0.525 +/- 0.075
	16.3	0.481 +/- 0.059
	17.1	0.473 +/- 0.072
Okumura [11]	13.4	0.530 +/- 0.036
	14.3	0.468 +/- 0.022
	15.0	0.423 +/- 0.019
Preiss & Fink [12]	14.8	0.144 +/- 0.057
Raics [10]	14.8	0.4545 +/- 0.02
Ribansky [8]	14.8	0.4729 +/- 0.03

Data exist from several sources for energies near 14 MeV [8 - 13]. These data are summarized in Table 2. Ribansky [8] gives an isomer ratio of 0.4729 at 14.8 MeV. Hudson [9] gives a ratio of 0.5015 at 14.8 MeV. Raics [10] gives data for energies from 13.52 to 14.8 MeV. His ratio at 14.8 MeV is 0.4545 +/- 0.02. The value at the SNL 14-MeV neutron generator, which has an average energy of 14.5 MeV, is seen from Table 1 to be 0.5405. This determination of the isomer production ratio has a significant uncertainty due to the large irradiation-decay correction (~25%) due to the fact that the exposure lasted for over six hours, the lack of early-time data due to the length of the irradiation and problems with rapid transportation to the counting laboratory, and the low-fluence exposure that led to poor statistics within the 10 min counting window.

Empirical Determination

Table 3 shows that the theoretical model of the energy-dependence of the $^{58m}Co/^{58t}Co$ isomer production ratio differs significantly from the measured spectrum-averaged isomer production ratios. In order to provide an alternative to the detailed experimental characterization of the isomer ratio in each neutron environment, the authors attempted to use the experimental data from the diverse range of neutron sources shown in Table 1 to "unfold" the energy-dependent isomer production ratio. The iterative spectrum unfolding code, SAND-II [14], was modified to perform the determination of the isomer production ratio. The basis functions for the "unfold" or solution projection were the product of the neutron fluence spectra for the environments in Table 1 [15] and the ENDF/B-VI $^{58}Ni(n,p)^{58t}Co$ cross section. The data to be fit were the isomer production ratios in column 2 of Table 1. The function to be determined is the energy-dependent isomer ratio. This methodology is similar to that used in traditional SAND-II spectrum determinations where the basis functions are dosimetry cross sections, the data to be fit are measured activities, and the function to be determined is the neutron spectrum. The initial trial function for the iterative determination of the $^{58m}Co/$

TABLE 3: Comparison of Fits for $^{58m}Co/^{58t}Co$ Isomer Production Ratio

Neutron Spectrum	Methodology For Modeling Energy-Dependence $^{58m}Co/^{58t}Co$ Isomer Production Ratio			
	Measured	Theoretical TNG	Iterative Fit	Recommended Function
SNL 14-MeV	0.5405	0.3838	0.5405	0.5399
$S^{3\,252}Cf$	0.2828	0.2413	0.2903	0.2996
SPR-III Central Cavity	0.3100	0.2374	0.2953	0.2952
ACRR Pb-B_4C Bucket	0.3220	0.2318	0.3080	0.2893
ACRR Central Cavity	0.2848	0.2329	0.2855	0.2900

^{58t}Co isomer ratio was chosen to be the TNG theoretical isomer production curve. Other trial functions were used in a methodology similar to the outer iteration methodology detailed in Reference 15.

Figure 3 shows the result of this empirical determination in the long-dashed curve labeled as "Iterative Fit Curve". The SAND-II methodology was found to be very insensitive to the shape of the trial isomer ratio; that is, SAND-II could not find areas of strong response to modify the energy-dependent shape of the trial isomer population. Figure 4 shows the relative response (cross section folded with the spectrum, the basis functions for the unfold) for the fission sources from Table 1. The response functions in this iterative unfold are seen to be very degenerate and unable to resolve structure in the isomer production ratio. The iterative fit seen in Figure 3 was the result of an external determination of a trial function after examining the spectral response shapes shown in Figure 4. The SAND-II code merely provided a normalization and was unable to significantly modify the shape. The iterative fit in Figure 3 differs too much in shape from the available mono-energetic experimental data to be given much credence. The small differences in spectral response shown in Figure 4 are numerical artifacts and either the cross section or spectral determinations were insufficiently accurate to provide a set of basis functions for unfolding the isomer ratio. For this unfolding approach to yield a valid result, data must be gathered from other spectra that show different energy-dependent shapes in the 3 to 9 MeV energy region. Data from $^{2}H(d,n)^{3}He$ and $^{7}Li(p,n)^{7}Be$ reactions would be very important additions to the spectra in Table 3 that are used in the empirical determination.

Suggested Ratio

The empirical "unfolding" of the energy-dependence of the isomer ratio proved to be unsatisfactory, even though it provided the best fit of the measured spectrum-averaged isomer ratios as shown in Table 3. Figure 3 shows a recommended ^{58m}Co/^{58t}Co isomer ratio that was derived by inspection of the available experimental data and the spectrum-averaged isomer measurements. An inspection rather than an "unfolding" was used because of conflicts in some of the experimental data and because of the inability of SAND-II-type iterative "unfolding" to properly treat the different assigned uncertainties in the experimental data. Table 3 shows that this recommended energy-dependent isomer production ratio fits the measured isomer ratios for a variety of environments to within about 5% in four of the five spectra. A 10% disagreement exists for the ACRR Pb-B_4C Bucket environment. Additional measurements of the isomer ratio and of the full spectrum characterization are being performed on this environment to try to resolve the disagreement.

Use of this empirical energy-dependent isomer ratio rather than a measured isomer ratio will lead to spectrum-averaged isomer ratios that have a larger uncertainty associated with them. Figure 5 shows the activity uncertainty that results when the isomer ratio uncertainty is coupled with the decay dynamics from Eqns. 3 and 4. The additional activity uncertainty is seen to start at less than half the isomer ratio uncertainty and rapidly decreases as the wait time between irradiation and counting increases. This methodology reduces to the normal activity measurement procedure, when the wait time has increased to four days, with no additional measurement uncertainty.

Implementation of Methodology at RML

As a result of this work the following procedure has been developed for implementation of short decay time nickel activity measurement at the Radiation Metrology Laboratory (RML).

- Count the nickel foil, but do not apply the usual counting-time decay corrections.
- Using the measured ^{58m}Co/^{58t}Co isomer production ratio, η_i, that is characteristic of the field, apply the correction for decay during irradiation from Eqns. 9 and 10 to obtain the isomer population ratio at the end of the irradiation

$$\xi_i(T_i) = \xi(T_{i2}) = \frac{N_a(T_{i2})}{N_a(T_{i2}) + N_b(T_{i2})} \qquad (14)$$

- Apply the correction for decay during the wait period between irradiation and counting from Eqns. 3 and 4 to obtain

$$\xi_p(T_w) = \frac{N_a(T_{c1})}{N_a(T_{c1}) + N_b(T_{c1})} \qquad (15)$$

- Use $\xi_p(T_w)$ to calculate Λ and ζ_b, the counting correction term for decay during count from Eqns. 12 and 13.
- Apply ζ_b to the measured nickel ground state activity to obtain a true ^{58t}Co activity measurement from the ^{58}Ni(n,p)^{58t}Co reaction.
- Determine the uncertainty in the ^{58m}Co/^{58t}Co spectrum-averaged isomer production ratio characteristic of this environment, ΔR_i. If a measurement process was used, experience suggests that this uncertainty is 2-3%. If the theoretical ^{58m}Co/^{58t}Co isomer production ratio from recommended curve in Figure 4 was folded in with a measured spectrum, experience suggests that the uncertainty may be up to 10%.
- Use the curve in Figure 5 and the time between the end of the irradiation and the start of counting to determine the effect a 1% uncertainty in the isomer production ratio has on the early-time measurement of ^{58}Ni(n,p)^{58}Co activity, $\Delta A_{1\%}$.
- Since the spectrum-averaged isomer production ratio uncertainty is linearly related to the early-time component of the activity uncertainty, multiply the result of the previous step by the actual isomer production ratio uncertainty. This term, $\Delta R_{early} = \Delta R_i \bullet \Delta A_{1\%}$, is added in quadrature with the other counting uncertainty terms and reported as part of the total activity uncertainty in the dosimetry report.

Conclusions

A methodology has been presented for the use of nickel monitor foils at short decay times. The recommended approach involves a measurement of the ^{58m}Co/^{58t}Co isomer ratio in the environment as well as the usual spectrum characterization. If good early-time data is available, the isomer production ratio can be obtained with a precision of 2-3%. This results in less than a 1.5% increase in the uncertainty of a nickel activation measurement even at the earliest times, decreasing to zero as the wait time between irradiation and counting increases.

If a measurement of the isomer ratio is not possible, a recommended energy-dependent curve is presented that can be folded with the neutron spectrum. This second approach results in an accuracy of ~10% in the isomer production ratio and an additional uncertainty in the nickel activation measurement of less than 5%, again decreasing to zero as the wait time between irradiation and counting increases.

Nomenclature

The following symbols are used in the mathematical formulation of the decay process:

λ_x	decay constant for state X, $\lambda_x = \ln(2)/\tau_x$.
$N_x(t)$	population of state X at time t measured relative to the end of irradiation.
$N_{x,i2}$	population of state X at the end of an irradiation.
P_x	production rate of state X.
t	time after the end of an irradiation.
t_i	time during an irradiation, measured relative to the start of the irradiation.
t_c	time during a foil activation count, measured relative to the start of the count.
$t_{x,mx}$	time of maximum population in nuclear state X.
T_{i1}	start time for a neutron irradiation.
T_{i2}	stop time for a neutron irradiation.
T_i	time of irradiation = $T_{i2} - T_{i1}$.
T_{c1}	start time for the counting of a foil activity.
T_{c2}	stop time for the counting of a foil activity.
T_c	time for the counting of a foil activity = $T_{c2} - T_{c1}$.

T_w	wait time between the stop of the irradiation and the start of the activity count $= T_{c1} - T_{i2}$.
τ_x	half-life of state X.
η_i	ratio of the isomer production rate of ^{58m}Co to $^{58t}Co = P_a/[P_a+P_b]$.
$\xi(t)$	ratio of the population of ^{58m}Co to ^{58t}Co at an absolute time t, $\xi(T_{c1}) = \xi_p(T_w)$.
$\xi_i(t_i)$	ratio of the population of ^{58m}Co to ^{58t}Co at time t during an irradiation, $\xi_i(t_i=0) = \eta_i$.
$\xi_p(t)$	ratio of the population of ^{58m}Co to the total ^{58t}Co activation at time t after an irradiation, $\xi_p(t=0) = \xi_i(t_i=T_i)$.
ζ_x	counting time correction to a measured activity for the population of state X.

The following values describe the nuclear data used in the above parent-daughter mathematical decay modeling for the $^{58}Ni(n,p)^{58}Co$ decay process:

subscript a	Parent nuclear state, $_{27}{}^{58}Co^{5+}$, metastable state, also denoted by ^{58m}Co.
subscript b	Daughter nuclear state, $_{27}{}^{58}Co^{2+}$, ground state, also denoted by ^{58g}Co.
^{58t}Co	The total ^{58}Co population, $^{58m}Co + {}^{58g}Co$.
τ_a	9.15 h
τ_b	1.706×10^{3} h
λ_a	0.07575 h^{-1}
λ_b	4.0758×10^{-4} h^{-1}

REFERENCES

[1] T. O. Passell, R. L. Heath, "Cross Sections of Threshold Reactions for Fission Neutrons: Nickel as a Flux Monitor," Nuclear Science and Engineering, Vol. 10, pp. 308-315, 1961.

[2] "Standard Test Method for Measuring Fast-Neutron Reaction Rates by Radioactivation of Sulfur-32, E265-87," Annual Book of ASTM Standards, Vol. 12.02, American Society for Testing and Materials, Philadelphia, PA, 19103.

[3] "Standard Test Method for Measuring Fast-Neutron Reaction Rates by Radioactivation of Nickel, E264-87," Annual Book of ASTM Standards, Vol. 12.02, American Society for Testing and Materials, Philadelphia, PA, 19103.

[4] Radiation Shielding Information Center, Oak Ridge National Laboratory, Peripheral Shielding Package PSR-298/TNG1.

[5] "ENDF-201, ENDF/B-VI Summary Documentation," edited by P. F. Rose, Brookhaven National Laboratory Report BNL-NCS-1741, 4th Edition, October 1991.

[6] C. Y. Fu, D. M. Hetrick, "Experience in Using the Covariances of Some ENDF/B-V Dosimetry Cross Sections: Proposed Improvements and Addition of Cross-Reaction Covariance," Proceedings of the Fourth ASTM-Euratom Symposium on Reactor Dosimetry: Radiation Metrology Techniques, Data Bases, and Standardization, Volume II, conference held at the National Bureau of Standards, Gaithersburg, Maryland on March 22-26, 1982, pp. 877 - 887, Report number NUREG/CP-0029, CONF-820321/V2.

[7] J. W. Meadows, J. F. Whalen, "$Ni^{58}(n,p)^{58m,g}Co$ Cross Section and Isomer Ratio from 1.04 to 2.67 MeV," Physical Review, Vol. 130, No. 5, pp. 2022-2025, 1963.

[8] I. Ribansky, J. Kristiak, L. Stoeva, C. Panteleev, "Neutron Activation Cross Section for Ni Isotopes at 14.8 MeV," Czech. J. Phys. B 35, pp 1128-1137, 1985.

[9] C. Hudson, "Neutron Excitation Functions For ^{45}Sc, ^{93}Nb, and ^{58}Ni in the Energy Range 13 - 19 MeV," Ann. Nucl. Energy, Vol. 5, pp. 589-595, 1978.

[10] P. Raics, Atomki Kozlem, Vol. 23, pp. 45, 1981.

[11] S. Okumura, "Isomer Pair Cross Sections By 13.4 - 15.0 MeV Neutrons," Nuclear Physics A93, pp. 74-80, 1967.

[12] I. L. Preiss, R. W. Fink, "New Isotopes of Cobalt: Activation Cross-Sections of Nickel, Cobalt, and Zinc For 14.8 MeV Neutrons," Nuclear Physics, 15, pp. 326-336, 1960.

[13] P. Decowski, W. Grochulski, A. Marcinkowski, K. Siwek, I. Siedzinska, Z. Wilhelmi, Nucl. Physics, A112, pp. 51, 1968.

[14] J. G. Kelly, D. W. Vehar, "Measurement of Neutron Spectra in Varied Environments by the Foil-Activation Method With Arbitrary Trials," SAND87-1330, Sandia National Laboratories, December 1987.

[15] W. N. McElroy, S. Berg, T. Crockett, and R. Hawkins, "A Computer-Automated Iterative Method for Neutron Flux Spectral Determination by Foil Activation," AFWL-TR-67-41, Vol. 1, Air Force Weapons Laboratory, Kirtland, New Mexico, July 1967.

Figure 2. Isomer Ratio in SPR-III Central Cavity

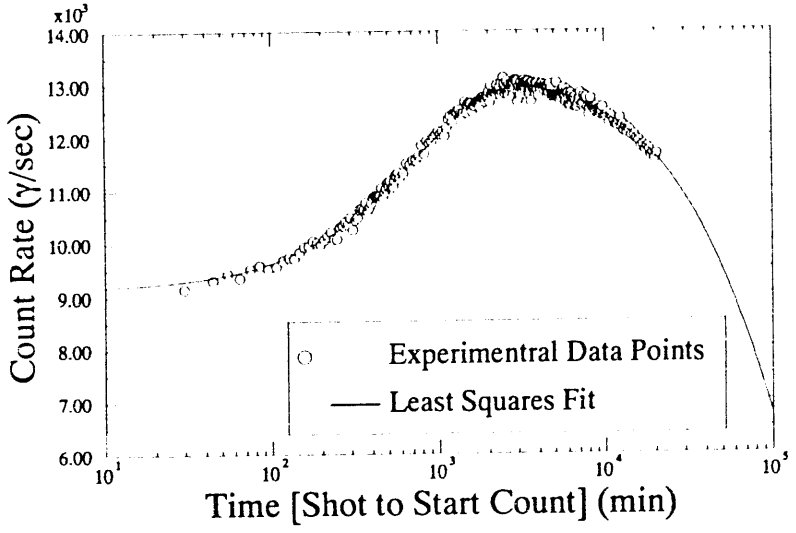

Figure 3. Comparison of Models for Isomer Ratio

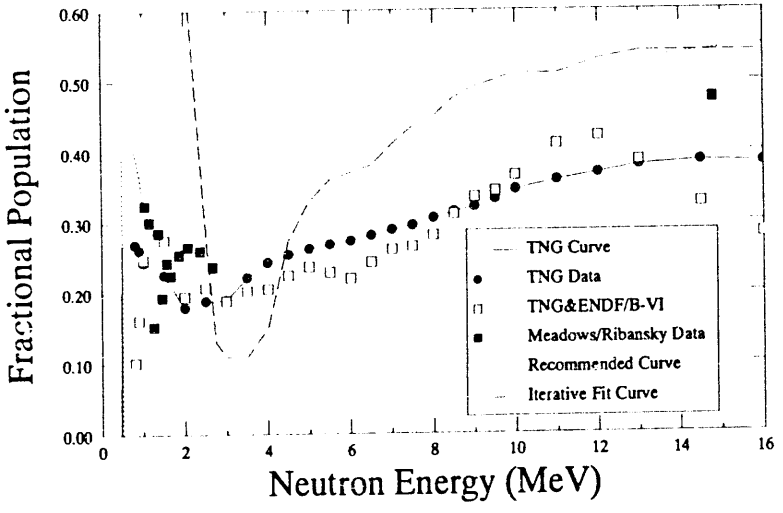

Figure 4. Spectral Response of $^{58}Ni(n,p)^{58}Co$ Sensor

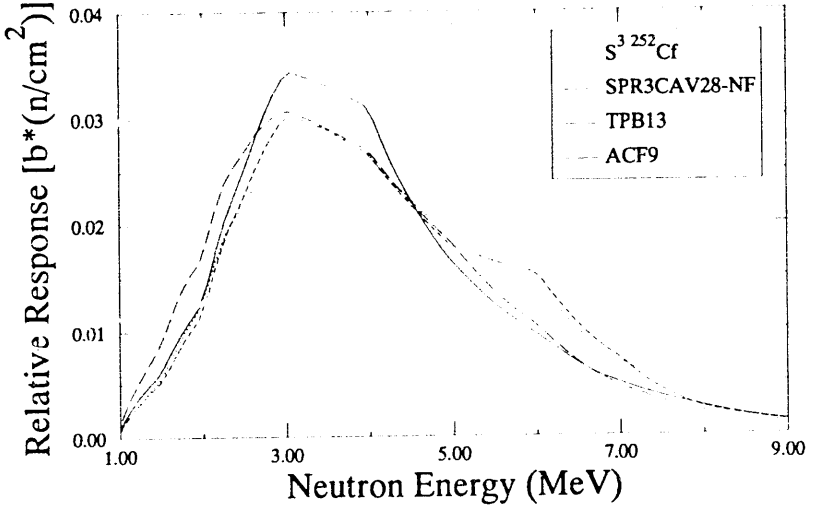

Figure 5. Effect of Change in Isomer Ratio on Activity

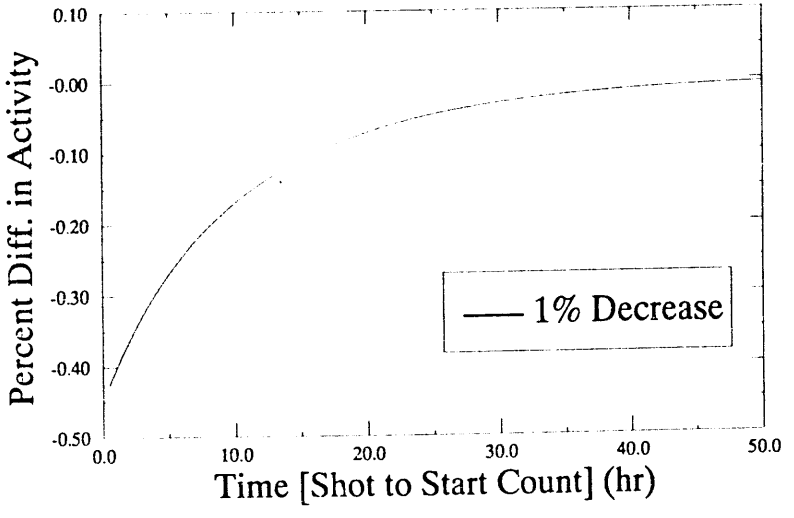

DATE
FILMED
12/8/93
END